PROTEIN STRUCTURE AND FOLDING:

A Stable Human p53 Heterotetramer Based on Constructive Charge Interactions within the Tetramerization Domain

Richard D. Brokx, Eleonora Bolewska-Pedyczak and Jean Gariépy

J. Biol. Chem. 2003, 278:2327-2332.
doi: 10.1074/jbc.M208528200 originally published online November 13, 2002

THE JOURNAL OF BIOLOGICAL CHEMISTRY
Vol. 278, No. 4, Issue of January 24, pp. 2327–2332, 2003
Printed in U.S.A.

A Stable Human p53 Heterotetramer Based on Constructive Charge Interactions within the Tetramerization Domain*

Received for publication, August 20, 2002, and in revised form, October 22, 2002
Published, JBC Papers in Press, November 13, 2002, DOI 10.1074/jbc.M208528200

Richard D. Brokx, Eleonora Bolewska-Pedyczak, and Jean Gariépy‡

From the Department of Medical Biophysics, University of Toronto, Toronto, Ontario M5G 2M9, Canada

The human p53 tetramerization domain (called p53tet; residues 325–355) spontaneously forms a dimer of dimers in solution. Hydrophobic interactions play a major role in stabilizing the p53 tetramer. However, the distinctive arrangement of charged residues at the dimer-dimer interface suggests that they also contribute to tetramer stability. Charge-reversal mutations at positions 343, 346, and 351 within the dimer-dimer interface were thus introduced into p53tet constructs and shown to result in the selective formation of a stable heterotetramer composed of homodimers. More precisely, mutants p53tet-E343K/E346K and p53tet-K351E preferentially associated with each other, but not with wild-type p53tet, to form a heterodimeric tetramer with enhanced thermal stability relative to either of the two components in isolation. The p53tet-E343K/E346K mutant alone assembled into a weakly stable tetramer in solution, whereas p53tet-K351E existed only as a dimer. Moreover, these mutants did not form heterocomplexes with wild-type p53tet, illustrating the specificity of the ionic interactions that form the novel heterotetramer. This study demonstrates the dramatic importance of ionic interactions in altering the stability of the p53 tetramer and in selectively creating heterotetramers of this protein scaffold.

Human p53 plays an important role in tumor suppression (1–4). It is a modular protein consisting of discrete functional domains, which can be expressed and studied in isolation. In particular, residues 325–355 of human p53 (p53tet) spontaneously form a tetramer in solution (see Fig. 1*a*) (5–7). Each monomer within the context of the p53tet domain adopts an identical structure, *viz.* a short N-terminal β-strand (residues 326–333) followed by a turn and a C-terminal α-helical domain (residues 335–354). Two monomers associate in an antiparallel fashion through contacts between β-sheet strands as well as hydrophobic interactions involving α-helical residues to form a "primary dimer" (6, 7). One significant salt bridge in the p53tet region occurs between Arg^{337} of one subunit and Asp^{352} of its adjacent subunit (side chain oxygen–nitrogen distance of 2.72 Å) (6), stabilizing the structure of the primary dimer (8, 9). Two primary dimers then self-associate through an interface derived from residues located in their α-helical domains to form a "dimer of dimers," referred to as a p53 tetramer. Mutations of amino acids at this interface have highlighted the importance of hydrophobic residues leading to the formation of the tetramer as well as stable p53 dimers (10–15). To date, knowledge relating to the contribution of charged residues at this interface to the nature and stability of the tetramer through ion pair formation remains minimal. In comparison, the impact of ion pairs on the oligomeric state and stability of other self-assembling peptide domains such as coiled-coil sequences is well documented. Naturally occurring and engineered coiled-coil domains have been shown to form homodimers as well as heterodimers (16–19) and heterotetramers (20). Protein complexes such as the Fos-Jun heterodimer (19), for example, occur as a result of charged groups in their coiled-coil regions, which promote hetero-oligomerization through the destabilization of homotypic interactions.

An examination of the crystal structure (6) of the human p53 tetramerization domain reveals the presence of one arginine (Arg^{342}), one lysine (Lys^{351}), and four glutamates (Glu^{339}, Glu^{343}, Glu^{346}, and Glu^{349}) within the boundaries of the dimer-dimer interface (residues 338–351). Of these residues, the only pairs of complementary charged side chains proximal enough to form an intermonomer salt bridge involve Lys^{351} with Glu^{343} and/or Glu^{346} (see Fig. 1*b*). The side chain oxygen of Glu^{343} on one monomer was found to be located 2.58 Å from the nitrogen side chain of Lys^{351} on another monomer. NMR structures of p53tet (7, 21) in solution have revealed that Glu^{346} is apparently closer than Glu^{343} to Lys^{351}, although these ionic residues are farther apart in these structures than in the crystal structure. Finally, alignment of the tetramerization domain sequences of p53 from *Xenopus laevis* (22) and rainbow trout (23) as well as of human p73 and p63 (24–26) (see Fig. 1*c*) indicates that the naturally occurring E343K mutation in their tetramerization domains is always coupled with a corresponding loss of the positively charged lysine residue at position 351. Taken together, these findings suggest that the presence of salt bridges involving Lys^{351} with Glu^{343} and/or Glu^{346} would contribute four or more ionic interactions within the context of the p53 tetramer interface, favoring the stabilization and self-association of primary dimers. To test this hypothesis, we engineered variants of the p53tet domain harboring charge-reversal mutations at positions 343, 346, and 351 (see Fig. 1*c*). Mutants p53tet-E343K, p53tet-E346K, and p53tet-E343K/E346K will result in dimer-dimer interfaces exhibiting a preponderance of positively charged side chains, whereas mutant p53tet-K351E will produce an interface enriched for negatively charged residues, both scenarios leading to electrostatic interactions unfavorable for tetramer formation. Conversely, the negative effects of introducing like charges at the dimer-dimer interface should be nullified in the case of heterotetramers composed of dimers of p53tet-K351E paired with p53tet-E343K, p53tet-E346K, or p53tet-E343K/E346K. The stability

* This work was supported by a grant from the Canadian Breast Cancer Research Initiative in association with the National Cancer Institute of Canada and the Canadian Cancer Society. The costs of publication of this article were defrayed in part by the payment of page charges. This article must therefore be hereby marked "*advertisement*" in accordance with 18 U.S.C. Section 1734 solely to indicate this fact.

‡ To whom correspondence should be addressed: Dept. of Medical Biophysics, University of Toronto, 610 University Ave., Toronto, Ontario M5G 2M9, Canada. Tel.: 416-946-2967; Fax: 416-946-6529; E-mail: gariepy@uhnres.utoronto.ca.

and oligomeric state of these p53tet constructs were analyzed in a series of biophysical experiments to resolve the role of such salt bridges at the dimer-dimer interface.

EXPERIMENTAL PROCEDURES

Mutagenesis—Plasmids pET-15b-p53-(310–360) and pET-15b-p53-(310–360)-M340Q/L344R (15) were gifts from the laboratory of Dr. Cheryl Arrowsmith (Ontario Cancer Institute). The plasmids contain a synthetic gene coding for residues 310–360 of human p53 inserted into the *Nde*I and *Bam*HI restriction sites of the bacterial expression vector pET-15b (Novagen, Madison, WI). The p53-(310–360) sequence is preceded by a vector-encoded His_6 metal ion affinity purification tag and a thrombin cleavage site (see Fig. 1*c*). The E343K, E346K, and K351E single mutants and the E343K/E346K double mutant of p53-(310–360) were assembled by PCR mutagenesis following a two-step three-primer method (27) using ProofStart DNA polymerase (QIAGEN, Mississauga, Ontario, Canada). PCR products were purified from reaction mixtures or agarose gels using QIAquick PCR purification and QIAquick gel extraction kits (QIAGEN). The final PCR products were cloned into a pET-15b vector. Mutations in the gene were confirmed by DNA sequencing. Plasmid constructs were transformed into competent BL21(DE3) pLysS cells (Novagen) according to standard methods (28).

Protein Expression and Purification—Wild-type and mutant His_6-p53-(310–360) (*i.e.* His_6-p53tet) proteins were expressed and purified by the same methods. Briefly, stocks of BL21(DE3) pLysS cells carrying the appropriate plasmid were plated on LB-agar plates supplemented with 100 μg/ml carbenicillin and 34 μg/ml chloramphenicol. A single colony was subsequently used to inoculate 40 ml of terrific broth supplemented with the same antibiotics. The cultures were grown overnight with shaking at 37 °C. A 15-ml aliquot of each culture was used to inoculate 1.5 liters of preheated (37 °C) terrific broth containing carbenicillin and chloramphenicol. The resulting cultures were then grown at 37 °C with shaking until $A_{600\ nm}$ = 0.6~0.9 (2–3 h), at which point 0.5 mM isopropyl-β-D-thiogalactopyranoside was added to the medium to induce protein expression. Cells were harvested by centrifugation after a 3-h induction period.

Cell pellets (~7.5 g, wet weight) were subjected to three freeze/thaw cycles and resuspended in ~3.7 volumes of buffer A (50 mM Tris-HCl, pH 8.0, 500 mM NaCl, and 0.1% Triton X-100) with 20 mM imidazole, 1 mM phenylmethylsulfonyl fluoride, 10 mM $MgCl_2$, and 2.5 units/ml Benzonase nuclease (Novagen). This suspension was placed on ice and sonicated three successive times for 45 s, and the resulting sonicate was centrifuged at 15,000 × *g* for 30 min. The supernatant was loaded onto a 2.5-ml column of Talon metal affinity resin (Clontech, Palo Alto, CA) equilibrated with buffer A containing 25 mM imidazole and 1 mM phenylmethylsulfonyl fluoride, and the resin was washed with 25–50 ml of the same buffer. Pure protein was eluted with 20 ml of buffer A containing 200 mM imidazole. The eluate was dialyzed extensively against 20 mM NH_4HCO_3, and the protein was lyophilized and stored at −20 °C until used. Purity was determined by SDS-PAGE with Coomassie staining (28) and matrix-assisted laser desorption ionization time-of-flight (MALDI-TOF)[1] mass spectrometry (Molecular Medicine Research Centre Mass Spectrometry Laboratory, University of Toronto).

Circular Dichroism Spectroscopy—CD spectra were recorded on an Aviv 62A DS circular dichroism spectrometer using a 0.5-cm path length rectangular cuvette with a 2-ml sample volume. Protein samples (10 μM) were prepared in sample buffer (25 mM sodium phosphate, pH 7.0, and 100 mM NaCl). Wavelength scans were recorded with a 1-nm spectral bandwidth (1 nm between points) and an averaging time of 8 s. Ellipticity measurements at 222 nm were collected as a function of temperature for each p53tet construct (or mixtures) using a 1-nm band width and a 50-s averaging time. Measurements were recorded from 20 to 98 °C at 3 °C intervals with a 1-min temperature pre-equilibration. Ellipticity values were plotted as the fraction of unfolded protein *versus* temperature assuming a two-state folding model.

Ultracentrifugation—Sedimentation equilibrium ultracentrifugation experiments were performed on a Beckman Optima XL-I analytical ultracentrifuge using an AN50-Ti rotor with six-channel charcoal-Epon cells. Protein concentrations were 0.125, 0.25, and 0.5 mg/ml prepared in sample buffer as measured by UV spectroscopy using the molar extinction coefficient for a free tyrosine residue ($\epsilon_{276\ nm}$ = 1450). Samples were centrifuged at 20 °C at three different speeds for 24 h before equilibrium absorbance measurements were taken at 230 nm. Association constants and molecular masses were estimated using Beckman XL-I data analysis software in which absorbance *versus* radial position data were fitted to the sedimentation equilibrium equation using non-linear least-squares techniques (29).

Size-exclusion Chromatography—Analytical size-exclusion chromatography (SEC) experiments were performed on a Superdex-75HR column (10 mm × 30 cm, Amersham Biosciences) operating at a flow rate of 1 ml/min. Samples (0.8 mg in 400 μl) were injected onto the column, and absorbance was monitored at 280 nm. The column was calibrated with gel filtration standards from Bio-Rad.

Thrombin Cleavage of Mutant p53tet Proteins—His_6-p53tet-E343K/E346K and His_6-p53tet-K351E were cleaved with thrombin using a thrombin cleavage capture kit (Novagen). Two milligrams of each protein were dissolved in 5 ml of 1× thrombin cleavage buffer (20 mM Tris-HCl, pH 8.4, 150 mM NaCl, and 25 mM $CaCl_2$). Biotinylated thrombin (0.5 units, 0.25 units/mg) was then added to the reaction mixture, and the reaction was left to proceed at room temperature for 16 h. The biotinylated thrombin was subsequently removed with streptavidin-agarose, and the cleaved His_6 tag was eliminated with Talon metal affinity resin. The filtrate containing pure cleaved p53tet-E343K/E346K or p53tet-K351E, without the His_6 tag, was dialyzed against 20 mM NH_4HCO_3, lyophilized, and stored at −20 °C until used. Samples were analyzed for cleavage and purity by SDS-PAGE. Complete cleavage was achieved, and cleavage at other sites in the protein did not occur, as no other low molecular mass bands were detected.

Metal Affinity Experiments—Lyophilized His_6-p53tet-WT, His_6-p53tet-E343K, His_6-p53tet-E346K, His_6-p53tet-E343K/E346K, His_6-p53tet-K351E, p53tet-E343K/E346K, and p53tet-K351E were dissolved in sample buffer to final concentrations of 0.2 mM (1.6 mg/ml). Combinations of p53tet constructs (at a molar equivalence of each construct) were mixed and incubated at room temperature for 1 h in microcentrifuge tubes. Fifty microliters of Talon metal affinity resin were added to 300 μl of each mixture, and the resulting samples were gently mixed at room temperature for 10 min. The resin was pelleted by centrifugation (10,000 × *g* for 30 s) and subsequently washed five times with 200 μl of sample buffer. Bound proteins were eluted in the presence of 100 μl of sample buffer containing 0.5 M imidazole. Samples corresponding to the original mixture of proteins prior to treatment with Talon resin as well as aliquots of the supernatant after incubation with Talon resin and of the eluate from the imidazole wash were analyzed by SDS-PAGE.

RESULTS

Design and Structure of Human p53tet Constructs—A wild-type human p53-(310–360) construct with an N-terminal His_6 tag and a thrombin cleavage site as well as four corresponding p53tet variants harboring mutation E343K, E346K, E343K/E346K, or K351E (Fig. 1*c*) were expressed in bacteria. The five 72-amino acid-long constructs were purified to homogeneity by metal affinity chromatography (cobalt-based Talon resin), and their masses were confirmed by MALDI-TOF mass spectrometry and SDS-PAGE. The CD spectra of the p53tet-E343K/E346K and p53tet-K351E analogs were similar to that of our p53tet-WT construct (data not shown), suggesting a comparable secondary structure.

Oligomeric State of p53tet Mutants—Wild-type and mutant p53tet constructs were subjected to analytical ultracentrifugation at 20 °C to assess their oligomeric state. Representative results are shown in Fig. 2. Data for all variants were fitted to a single species; the apparent masses are listed in Table I and indicate that p53tet-WT (apparent mass of 31.8 kDa) is a tetramer in solution. The analog p53tet-E343K/E346K is also predominantly a tetramer. However, its apparent oligomeric state (3.5) is lower than that of p53tet-WT (3.9), suggesting that the p53tet-E343K/E346K tetramer is less stable than its p53tet-WT counterpart. The data for p53tet-WT and p53tet-E343K/E346K can best be analyzed by assuming a monomer-tetramer equilibrium. The free energy change upon tetramerization (ΔG^0) for p53tet-WT was calculated to be −23.4 kcal/mol, which corresponds to a K_d (total protein concentration at which half the protein exists as a tetramer) of 2.0 μM. This agrees well with published values for similar p53tet peptides (30, 31). Using the same data treatment, the ΔG^0 for tetramer formation of p53tet-E343K/E346K was found to be −20.0 kcal/

[1] The abbreviations used are: MALDI-TOF, matrix-assisted laser desorption ionization time-of-flight; SEC, size-exclusion chromatography; WT, wild-type.

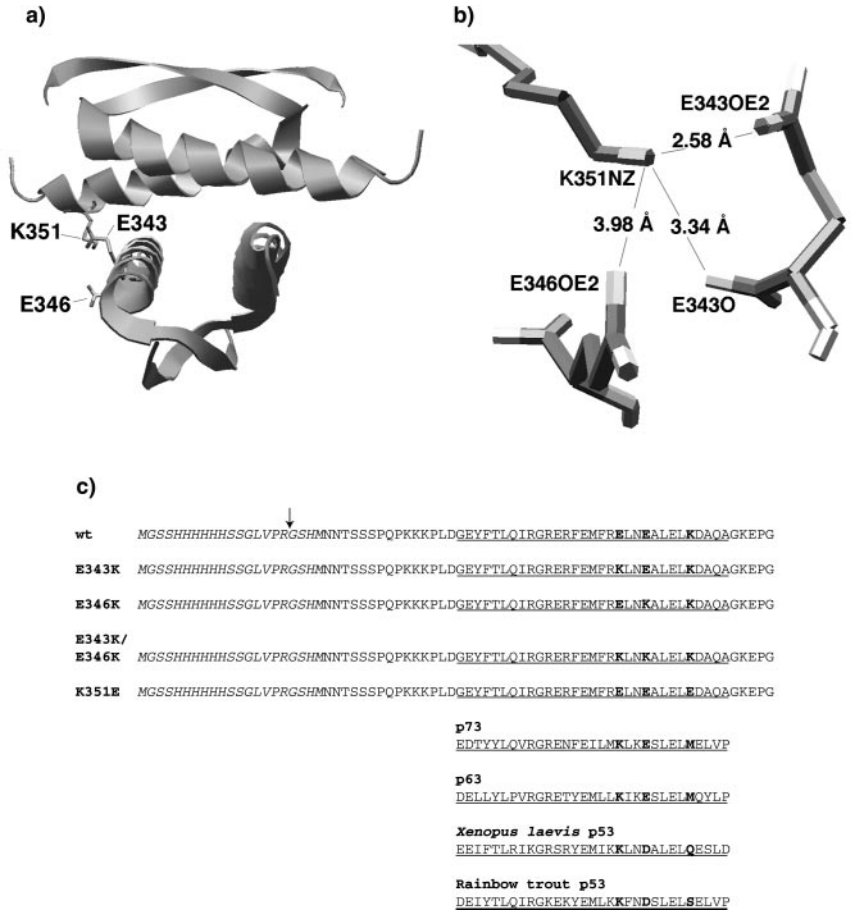

FIG. 1. **Structure of the tetramerization domain of human p53.** *a*, three-dimensional structure of the tetramerization domain of human p53 as determined by x-ray crystallography (Protein Data Bank code 1c26) (6) using Swiss PDB Viewer (available at www.expasy.ch/spdv) (35). One ionic network involving Glu^{343}, Glu^{346}, and Lys^{351} is depicted as a wire-frame model. *b*, close-up view of the ionic network. Relevant distances between atoms are indicated. *c*, sequences of the 72-amino acid-long p53tet protein constructs used in this study. Vector-associated sequences (histidine tag and thrombin cleavage site) are shown in *italics*, and the p53tet minimum structural domain (residues 325–355 of human p53) is *underlined*. Glu^{343}, Glu^{346}, and Lys^{351} are shown in *boldface*. The site of thrombin cleavage is indicated by an *arrow*. Alignment (performed with ClustalW) (36) of sequences of the tetramerization domains of human p73 (24) and p63 (26) as well as of p53 proteins from *X. laevis* (22) and rainbow trout (23) is presented to highlight compensatory mutations involving Glu^{343} and Lys^{351}, which avoid unfavorable charge effects.

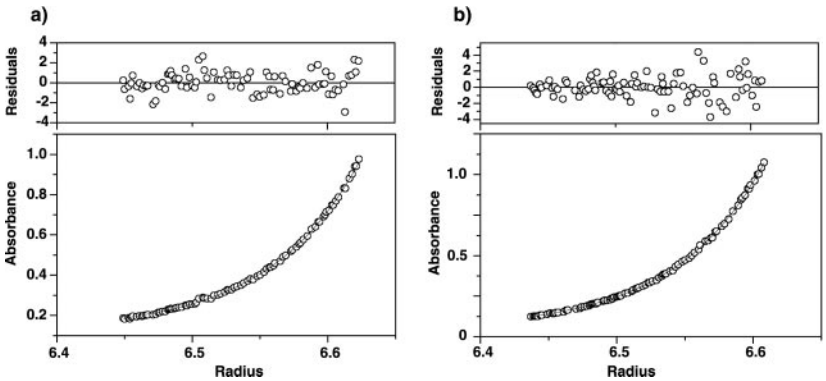

FIG. 2. **Representative sedimentation equilibrium ultracentrifugation data for p53tet variants, measured at 20 °C at the indicated speeds.** *a*, p53tet-K351E (33,000 rpm); *b*, p53tet-E343K/E346K + p53tet-K351E (32,000 rpm). Absorbance measurements were taken at 230 nm. The fit for *a* is to a monomer-dimer equilibrium; the fit for *b* is a free fit to a single oligomeric species. Residuals are multiplied by 10^3 for clarity.

TABLE I
Apparent mass and oligomeric state of p53tet constructs derived from sedimentation equilibrium ultracentrifugation studies

p53tet variant	Apparent molecular mass	Apparent molecular mass/ monomer molecular mass[a]
	kDa	
WT	31.8	3.9
E343K/E346K	29.1	3.5
K351E	16.4	2.0
E343K/E346K + K351E	31.9	3.9

[a] Apparent molecular mass/monomer molecular mass is referred to as the apparent oligomeric state of the protein; the molecular mass of the p53tet constructs used is 8.15 kDa.

mol, which corresponds to a K_d of 13.3 μM. Thus, these calculations confirm the decreased stability of p53tet-E343K/E346K relative to p53tet-WT. The apparent oligomeric state of p53tet-K351E was calculated to be 2.0, indicating that this mutant is a dimer in solution. Data were also fitted to a monomer-dimer equilibrium; the K_d was calculated to be very low ($<10^{-15}$ M).

The oligomeric state of the p53tet mutants was further confirmed by SEC. Representative elution profiles are depicted in Fig. 3. Under these conditions, the tetrameric p53tet-WT construct eluted at 10.3 min as a tetramer with an apparent molecular mass of 44.3 kDa. As has been noted previously (10, 12), the observed value is greater than the expected molecular mass for tetrameric p53tet-WT because of the relatively unique nature of its tetrameric structure. p53tet-M340Q/L344R, which is known to form dimers (15), eluted at 11.5 min, establishing the retention time for a dimeric form of such constructs. p53tet-E343K, p53tet-E346K, and p53tet-E343K/E346K (Fig. 3) eluted at times similar to p53tet-WT, indicating that these mutants exist as tetramers. The analog p53tet-K351E eluted at 11.3 min, pointing out that this construct, as in the case of p53tet-M340Q/L344R, is a dimer. This finding supports our

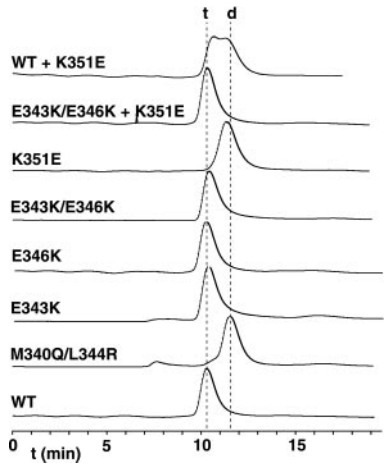

FIG. 3. **Molecular size of p53tet variants.** Variants of human p53tet were analyzed by SEC. Injected samples (0.8 mg in 400 μl) were dissolved in sample buffer, and absorbance was recorded at 280 nm. *Dashed lines* indicate the elution times of the p53tet-WT tetramer (*t*) and of the known p53tet-M340Q/L344R dimer (*d*). The elution profiles of the p53tet-E343K + p53tet-K351E and p53tet-E346K + p53tet-K351E mixtures (not shown) are also similar to that of p53tet-WT.

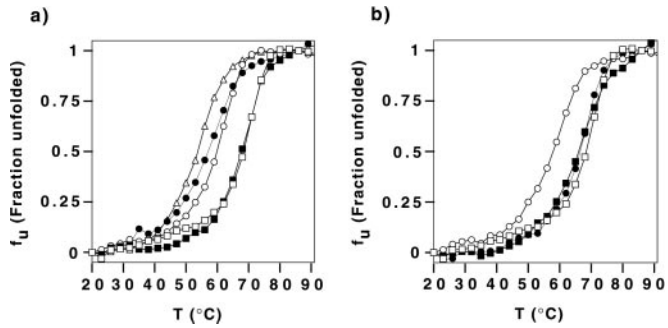

FIG. 4. **Thermal stability of p53tet variants.** Temperature melting curves for individual p53tet constructs and various combinations were determined by plotting ellipticity values derived from CD measurements at 222 nm as the fraction of unfolded protein (f_u) *versus* temperature, assuming a two-state folding model. Experiments were conducted with a protein (monomer) concentration of 10 μM in sample buffer. *a*, p53tet mutants compared with p53tet-WT. □, p53tet-WT; ■, p53tet-E343K; ○, p53tet-E346K; ●, p53tet-E343K/E346K; △, p53tet-K351E. *b*, mixtures of p53tet mutants. □, p53tet-WT; ■, p53tet-E343K + p53tet-K351E; ○, p53tet-E346K + p53tet-K351E; ●, p53tet-E343K/E346K + p53tet-K351E.

TABLE II
T_m of p53tet constructs derived from CD studies

p53tet variant	T_m
	°C
WT	68
E343K	67
E346K	60
E343K/E346K	57
K351E	53
E343K + K351E	66
E346K + K351E	58
E343K/E346K + K351E	66

analytical ultracentrifugation results (see above).

p53tet Constructs with Charge Inversions at Positions 351 and 343/346 Are Less Stable—As shown above, the sedimentation equilibrium ultracentrifugation data indicated that the p53tet-E343K/E346K tetramer was less stable than p53tet-WT, with a difference in ΔG^0 for tetramerization of 3.4 kcal/mol. In addition, CD was used to measure the thermal stability of wild-type and mutant forms of p53tet. All constructs displayed a sigmoidal unfolding curve, which is indicative of cooperative unfolding. Under the conditions of this study (25 mM sodium phosphate, 100 mM NaCl, and 10 μM each p53 construct based on monomer concentration), p53tet-WT had a thermal unfolding temperature (T_m) of 68 °C.

The effect of temperature on the fraction of folded structure as calculated from changes in ellipticity at 222 nm (Fig. 4 and Table II) suggested that the inversion of charges at residues 343, 346, and 351 resulted in less stable tetramers. The E343K and E346K mutations both posted lower T_m values in relation to the p53tet-WT construct. The E346K mutation had a greater effect on T_m (60 °C) than the identical mutation at position 343 (E343K; 67 °C). When both E343K and E346K mutations were included, the destabilizing effect was greater (T_m = 57 °C). The K351E mutation to p53tet alone displayed the largest destabilizing effect (T_m = 53 °C), demonstrating an important role for Lys^{351} in stabilizing the tetramer.

p53tet-K351E and p53tet-E343K/E346K Specifically Form a Heterotetramer—Because p53tet-K351E forms a dimer in solution, it can be used to study the formation of heterotetramers with other p53tet species. SEC results showed that when p53tet-K351E was mixed at equal proportions with p53tet-E343K (data not shown), p53tet-E346K (data not shown), or p53tet-E343K/E346K (Fig. 3), the result was a single peak corresponding to a tetrameric species. This finding indicates that p53tet-K351E associates with these mutants to form a 2:2 heterotetramer. This association is specific. For instance, p53tet-K351E did not associate with p53tet-WT, as demonstrated by the elution profile of an equimolar mixture of these two proteins (Fig. 3). Two peaks were observed for this mixture, with elution times very similar to those of the individual p53tet components (10.5 min for the wild-type tetramer and 11.2 min for the K351E dimer). The substantial amount of dimeric species in the size-exclusion elution profile of the mixture of p53tet-K351E and p53tet-WT indicated that an association of p53tet-WT with p53tet-K351E did not occur.

Sedimentation equilibrium ultracentrifugation data (Fig. 2 and Table I) also showed that an equimolar mixture of p53tet-E343K/E346K and p53tet-K351E produced a new species that occurred as a tetramer (single-state free fit revealed an apparent oligomeric state of 3.9, identical to that of p53tet-WT). Importantly, both SEC and ultracentrifugation showed the absence of any dimeric species, suggesting that no uncomplexed p53tet-K351E remains in solution after mixing. A fit of the ultracentrifugation data for the p53tet-E343K/E346K + p53tet-K351E mixture to a monomer-tetramer equilibrium revealed an apparent ΔG^0 for tetramerization of −23.5 kcal/mol, which corresponds to a K_d of 1.8 μM. Due to the complex nature of the mixture (monomers, homodimers, homotetramers, and heterotetramers could all potentially be present), the significance of these values is open to question. However, the close correspondence between the ΔG^0 and K_d values obtained and those observed for p53tet-WT (ΔG^0 = −23.4 kcal/mol, K_d = 2.0 μM) suggests that the stability of the heterotetramer is similar to that of p53tet-WT.

The temperature melting curves derived from CD spectra (Fig. 4*b*) precisely demonstrated that the increased stability associated with this heterotypic interaction was much more dramatic with the E343K/E346K double mutant than with either p53tet-E343K or p53tet-E346K alone. The temperature curves presented in Fig. 4 show that when p53tet-E343K or p53tet-E346K was combined with p53tet-K351E, the melting temperatures of the resulting mixtures (Table II) were lowered relative to the Glu-to-Lys single mutant alone (T_m = 66 °C for p53tet-E343K + p53tet-K351E *versus* 67 °C for p53tet-E343K, T_m = 58 °C for p53tet-E346K + p53tet-K351E *versus* 60 °C for p53tet-E346K). This finding indicates a lack of a stabilizing interaction between these p53tet components. In contrast, Fig.

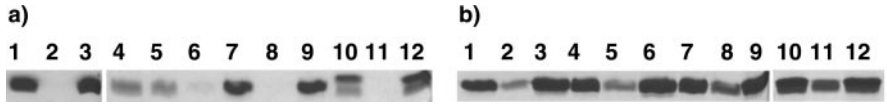

FIG. 5. **Metal affinity of p53tet complexes.** Combinations of His_6-tagged and untagged p53tet complexes captured using metal affinity resin (Talon) were analyzed by SDS-PAGE. For each pair of p53tet constructs tested, the first lane represents the mixture of both components prior to the addition of Talon resin; the second lane is an aliquot of the supernatant after incubation with Talon resin; and the third lane depicts the eluate recovered in the presence of imidazole. *a*: *lanes 1–3*, His_6-p53tet-E343K/E346K and His_6-p53tet-K351E; *lanes 4–6*, p53tet-E343K/E346K and p53tet-K351E; *lanes 7–9*, His_6-p53tet-E343K/E346K and p53tet-K351E; *lanes 10–12*, p53tet-E343K/E346K and His_6-p53tet-K351E. *b*: *lanes 1* and *3*, His_6-p53tet-E343K and p53tet-K351E; *lanes 4–6*, His_6-p53tet-E346K and p53tet-K351E; *lanes 7–9*, His_6-p53tet-WT and p53tet-K351E; *lanes 10–12*, His_6-p53tet-WT and p53tet-E343K/E346K.

4 and Table II show that when p53tet-E343K/E346K and p53tet-K351E were combined, the result was a new species with a T_m of 66 °C. This temperature was dramatically higher than that of either of the two mutants alone (57 °C for p53tet-E343K/E346K and 53 °C for p53tet-K351E) and nearly equal to the value observed for p53tet-WT (68 °C). These CD unfolding results support the sedimentation equilibrium ultracentrifugation data, which also suggested that the stability of the heterotetramer is similar to that of the p53tet-WT tetramer.

Selective Capture of His_6-tagged p53tet Complexes on a Metal Affinity Resin Demonstrates the Existence of Heterotetramers—The specific heterotypic association of p53tet-E343K/E346K and p53tet-K351E was further assessed by monitoring the binding of protein complexes composed of His_6-tagged and untagged p53tet constructs to cobalt-bound affinity resin (Talon). The resulting band patterns observed by SDS-PAGE (Fig. 5) provide a unique signature describing the nature of the complexes formed. Fig. 5*a* shows the results of combining together p53tet-E343K/E346K and p53tet-K351E. *Lanes 1–3* clearly show that His_6-p53tet-E343K/E346K and His_6-p53tet-K351E together specifically bound Talon resin (*lane 2*, no band), but were eluted with a high concentration of imidazole (*lane 3*). As expected, neither of the p53tet constructs lacking the His_6 tag (*lanes 4–6*) was able to bind to the metal affinity resin. (Protein bands were found in the wash fraction (*lane 5*).) p53tet-E343K/E346K migrated slightly faster than p53tet-K351E upon SDS-PAGE, such that His_6-p53tet-E343K/E346K ran at the same position as cleaved p53tet-K351E (*lane 7*). When this mixture was bound to the affinity resin, both species bound to the resin (*lane 8*, no band), and both species were eluted with imidazole (*lane 9*). This finding demonstrates the specific association of these two proteins to form a complex with affinity for metal ions. The reciprocal combination yielded the same result, *i.e.* the association of cleaved p53tet-E343K/E346K and His_6-p53tet-K351E resulted in a complex retained by the metal-bound resin (*lanes 10–12*). In this case, separate bands for the two species can be clearly seen due to the differences in their electrophoretic mobilities.

The temperature melting curves for various p53tet combinations (Fig. 4) indicate that the formation of a heterotetramer with p53tet-K351E was most specific and strongest for the E343K/E346K double mutant. These findings are also supported by the results from metal affinity capture experiments. As Fig. 5*b* shows, His_6-p53tet-E343K and His_6-p53tet-E346K both interacted with p53tet-K351E, resulting in the retention of p53tet-K351E on the Talon matrix (*lanes 1–3* and *4–6*, respectively). However, both experiments yielded a significant amount of cleaved p53tet-K351E in the wash fractions (*lanes 2* and *5*). This was almost as much as when a mixture of His_6-p53tet-WT and cleaved p53tet-K351E was evaluated (*lanes 7–9*). More importantly, *lanes 10–12* show that His_6-p53tet-WT did not bind to cleaved p53tet-E343K/E346K either, as a substantial amount of this protein was also found in the unbound fraction. Thus, p53tet-E343K/E346K and p53tet-K351E form heterotetramers with each other, but not with p53tet-WT.

DISCUSSION

The tetramerization domain of human p53 is an important part of this key tumor suppressor protein. Analysis of the dimer-dimer interface of the human p53 tetramerization domain suggests that ion pair interactions between Glu^{343}, Glu^{346}, and Lys^{351} may contribute significantly to the stability of the tetramer. This hypothesis was further supported by the fact that the tetramerization domain sequences of p53 in other organisms as well as of human p63 and p73 (Fig. 1*c*) display the naturally occurring E343K mutation. This mutation is always coupled with a corresponding loss of the positively charged lysine residue at position 351. This hypothesis was tested by designing and analyzing variants of the tetramerization domain of human p53, *viz.* p53tet-E343K, p53tet-E346K, p53tet-E343K/E346K, and p53tet-K351E, harboring charge-reversal mutations at ionic residues.

In the first part of this study, the oligomeric state of these p53tet mutants was evaluated (Fig. 3 and Table I) to determine whether these mutations, as is the case with many mutations of hydrophobic residues in the dimer-dimer interface (10, 12, 15), change the oligomerization specificity of p53tet from a tetramer to a dimer. Indeed, it was revealed that p53tet-K351E is a dimer in solution, demonstrating that a single mutation to a charged residue is sufficient to produce dimeric p53. This finding confirms our hypothesis that the introduction of a charge-reversal mutation (Lys to Glu) at position 351 of the p53tet domain introduces non-constructive charge repulsions at the dimer-dimer interface.

In the next part of this study, the stability of the resulting p53tet mutants was evaluated. It has been established that the oligomeric state and folding pattern of the p53 tetramerization domain are tightly linked features of this protein scaffold, with the monomeric form being essentially unfolded (10, 13, 32). Thus, thermal unfolding patterns as measured by CD represent an indicator of the tendency of the p53tet domain to oligomerize. As expected for a tetrameric protein, the T_m of p53tet is dependent on protein concentration (10, 32). A p53 monomer concentration of 10 μM was thus selected for p53tet-WT to be fully unfolded at 98 °C, allowing us to compare T_m values between p53tet-WT and its variants. The T_m of p53tet is also dependent on the length of the protein or peptide used (10). However, the observed T_m of 68 °C for the 72-amino acid-long p53tet-WT construct used in this study is comparable to published values for related p53 constructs analyzed under these conditions (9, 10, 32). The thermal unfolding results shown in Fig. 4 revealed that p53tet-E346K was less stable than p53tet-E343K, suggesting that Glu^{346} is involved in a more pronounced stabilizing interaction at the dimer-dimer interface. Glu^{346} (rather than Glu^{343}) may thus more strongly interact with Lys^{351}, in contrast with predictions arising from the crystal structure (6). CD thermal unfolding studies showed that p53tet-K351E, in addition to being a dimer, was also very unstable, suggesting that the charge at position 351 is an important determinant of the stability of the p53 tetramer.

Subsequent experiments were undertaken to determine the

potential of these p53tet mutants to form heterotetramers. SEC (Fig. 3) and analytical ultracentrifugation (Table I) data both indicated that either the E343K or E346K mutation was sufficient to produce a species that specifically formed heterotetramers with p53tet-K351E. However, CD data (Fig. 4 and Table II) suggested that when both E343K and E346K mutations were included, the resulting heterotetramer with p53tet-K351E was much more stable relative to the two individual components. The specificity of the heterotetramer between p53tet-E343K/E346K and p53tet-K351E was also confirmed by metal affinity experiments (Fig. 5), which strikingly depicted the necessity of both Glu-to-Lys mutations in determining the specificity of the heterotetramer. It was also found that these two mutants specifically associated with each other, and not with wild-type human p53tet. This interesting finding suggests that human p53 mutants containing such mutations would indeed not have a 'dominant-negative' effect on cellular transformation because their intracellular expression would not directly compete or exchange with existing cellular pools of wild-type human p53 (33, 34). This study demonstrates for the first time the important contribution of ionic interactions involving Glu^{343}, Glu^{346}, and Lys^{351} to the stability of the dimer-dimer interface of the human p53tet domain.

Acknowledgments—We thank Dr. Cheryl Arrowsmith for providing the pET-15b-p53-(310–360) plasmid and the pET-15b-p53-(310–360)-M340Q/L344R mutant plasmid used in this study and for critical review of this manuscript. Sandy Go and Dr. Avi Chakrabartty are acknowledged for performing the analytical ultracentrifugation experiments.

REFERENCES

1. Lane, D. P. (1992) *Nature* **358,** 15–16
2. Arrowsmith, C. H., and Morin, P. (1996) *Oncogene* **12,** 1379–1385
3. Bargonetti, J., and Manfredi, J. J. (2002) *Curr. Opin. Oncol.* **14,** 86–91
4. Somasundaram, K. (2000) *Front. Biosci.* **5,** D424–D437
5. Chene, P. (2001) *Oncogene* **20,** 2611–2617
6. Jeffrey, P. D., Gorina, S., and Pavletich, N. P. (1995) *Science* **267,** 1498–1502
7. Lee, W., Harvey, T. S., Yin, Y., Yau, P., Litchfield, D., and Arrowsmith, C. H. (1994) *Nat. Struct. Biol.* **1,** 877–890
8. Davison, T. S., Yin, P., Nie, E., Kay, C., and Arrowsmith, C. H. (1998) *Oncogene* **17,** 651–656
9. DiGiammarino, E. L., Lee, A. S., Cadwell, C., Zhang, W., Bothner, B., Ribeiro, R. C., Zambetti, G., and Kriwacki, R. W. (2002) *Nat. Struct. Biol.* **9,** 12–16
10. Mateu, M. G., and Fersht, A. R. (1998) *EMBO J.* **17,** 2748–2758
11. Mateu, M. G., and Fersht, A. R. (1999) *Proc. Natl. Acad. Sci. U. S. A.* **96,** 3595–3599
12. McCoy, M., Stavridi, E. S., Waterman, J. L., Wieczorek, A. M., Opella, S. J., and Halazonetis, T. D. (1997) *EMBO J.* **16,** 6230–6236
13. Mateu, M. G., Sanchez Del Pino, M. M., and Fersht, A. R. (1999) *Nat. Struct. Biol.* **6,** 191–198
14. Noolandi, J., Davison, T. S., Volkel, A. R., Nie, X., Kay, C., and Arrowsmith, C. H. (2000) *Proc. Natl. Acad. Sci. U. S. A.* **97,** 9955–9960
15. Davison, T. S., Nie, X., Ma, W., Lin, Y., Kay, C., Benchimol, S., and Arrowsmith, C. H. (2001) *J. Mol. Biol.* **307,** 605–617
16. Graddis, T. J., Myszka, D. G., and Chaiken, I. M. (1993) *Biochemistry* **32,** 12664–12671
17. Lavigne, P., Kondejewski, L. H., Houston, M. E., Jr., Sonnichsen, F. D., Lix, B., Skyes, B. D., Hodges, R. S., and Kay, C. M. (1995) *J. Mol. Biol.* **254,** 505–520
18. Lumb, K. J., and Kim, P. S. (1995) *Biochemistry* **34,** 8642–8648
19. O'Shea, E. K., Rutkowski, R., and Kim, P. S. (1992) *Cell* **68,** 699–708
20. Fairman, R., Chao, H. G., Lavoie, T. B., Villafranca, J. J., Matsueda, G. R., and Novotny, J. (1996) *Biochemistry* **35,** 2824–2829
21. Clore, G. M., Ernst, J., Clubb, R., Omichinski, J. G., Kennedy, W. M., Sakaguchi, K., Appella, E., and Gronenborn, A. M. (1995) *Nat. Struct. Biol.* **2,** 321–333
22. Soussi, T., Caron de Fromentel, C., Mechali, M., May, P., and Kress, M. (1987) *Oncogene* **1,** 71–78
23. Caron de Fromentel, C., Pakdel, F., Chapus, A., Baney, C., May, P., and Soussi, T. (1992) *Gene* (*Amst.*) **112,** 241–245
24. Kaghad, M., Bonnet, H., Yang, A., Creancier, L., Biscan, J. C., Valent, A., Minty, A., Chalon, P., Lelias, J. M., Dumont, X., Ferrara, P., McKeon, F., and Caput, D. (1997) *Cell* **90,** 809–819
25. Davison, T. S., Vagner, C., Kaghad, M., Ayed, A., Caput, D., and Arrowsmith, C. H. (1999) *J. Biol. Chem.* **274,** 18709–18714
26. Yang, A., Kaghad, M., Wang, Y., Gillett, E., Fleming, M. D., Dotsch, V., Andrews, N. C., Caput, D., and McKeon, F. (1998) *Mol. Cell* **2,** 305–316
27. Landt, O., Grunert, H. P., and Hahn, U. (1990) *Gene* (*Amst.*) **96,** 125–128
28. Sambrook, J., Fritsch, E. F., and Maniatis, T. (1989) *Molecular Cloning: A Laboratory Manual*, 2nd Ed., Cold Spring Harbor Laboratory, Cold Spring Harbor, NY
29. Johnson, M. L., Correia, J. J., Yphantis, D. A., and Halvorson, H. R. (1981) *Biophys. J.* **36,** 575–588
30. Sakaguchi, K., Sakamoto, H., Lewis, M. S., Anderson, C. W., Erickson, J. W., Appella, E., and Xie, D. (1997) *Biochemistry* **36,** 10117–10124
31. Sakamoto, H., Lewis, M. S., Kodama, H., Appella, E., and Sakaguchi, K. (1994) *Proc. Natl. Acad. Sci. U. S. A.* **91,** 8974–8978
32. Johnson, C. R., Morin, P. E., Arrowsmith, C. H., and Freire, E. (1995) *Biochemistry* **34,** 5309–5316
33. Chene, P., and Bechter, E. (1999) *J. Mol. Biol.* **286,** 1269–1274
34. Shaulian, E., Zauberman, A., Ginsberg, D., and Oren, M. (1992) *Mol. Cell. Biol.* **12,** 5581–5592
35. Guex, N., and Peitsch, M. C. (1997) *Electrophoresis* **18,** 2714–2723
36. Thompson, J. D., Higgins, D. G., and Gibson, T. J. (1994) *Nucleic Acids Res.* **22,** 4673–4680